

Synergistic effect of different basalt fillers and annealing on the structure and properties of polylactide composites

Mateusz Barczewski^{a,*}, Olga Mysiukiewicz^a, Danuta Matykiewicz^a, Arkadiusz Kloziński^b, Jacek Andrzejewski^a, Adam Piasecki^c

^a Poznan University of Technology, Faculty of Mechanical Engineering, Institute of Materials Technology, Piotrowo 3, 61-138, Poznan, Poland

^b Poznan University of Technology, Institute of Chemical Technology and Engineering, Berdychowo 4, 60-965, Poznan, Poland

^c Poznan University of Technology, Faculty of Materials Engineering and Technical Physics, Institute of Materials Engineering, Piotrowo 3, 61-138, Poznan, Poland

ARTICLE INFO

Keywords:

PLA
Composite
Basalt
Fibers
Inorganic filler
Thermal treatment

ABSTRACT

The paper presents a study of the thermomechanical behavior of polylactide (PLA) composites filled with two different types of basalt fillers: micrometric basalt fibers (BMF) and basalt powder (BP) incorporated into the polymeric matrix with the amount of 5, 10 and 20 wt%. The composites were manufactured by melt processing and subjected to the annealing process in order to obtain a highly crystalline structure without the addition of nucleating agents. We found a remarkable enhancement of the thermomechanical stability of polylactide-based composites filled with basalt powder (BP) and micrometric basalt fibers (BMF) in the case of use of the thermal post-processing procedure. Despite a relatively low nucleation ability of the fillers on PLA, their presence in the case of annealed PLA-samples caused an additional increase up to 15 °C of the heat deflection temperature. The BP-filled composites reveal comparable thermomechanical properties improvement to BMF-filled composites, with higher resistance to adhesion loss in the polymer-filler interface during annealing.

1. Introduction

Polylactide or poly(lactic acid) (PLA) plays the dominant role in the market of biodegradable polymeric materials, finding the widest range of applications [1,2]. Its beneficial mechanical properties, good processability, the ability to undergo biodegradation in industrial conditions, as well as low cost and high availability, attract the interest of scientists and industry-associated researchers [3–5]. One of the most extensively researched fields related to PLA is the development of the production technology of composites based on it [6]. The application of both organic and inorganic fillers, including waste materials and by-products, allows to modify the properties of the biodegradable polymeric matrix thanks to complex interactions, including reinforcing effects and toughening resulting from the presence of rigid particles and the modification of macromolecular PLA structure [7–12].

One of the most significant disadvantages of PLA, which strongly suppresses its application as a construction material, is its poor ability to form a crystalline structure and the resulting relatively low thermomechanical stability (glass transition temperature $T_g \sim 60$ °C). The overall mechanical and thermomechanical properties of PLA are

strongly dependent on polymer crystallinity as well as molecular weight. Most of the commercially available PLA grades are polymers characterized by a relatively low crystallization rate [13]. It should be mentioned that even the addition of various nucleating agents such as talc, aromatic sulfonate derivatives or poly-D-lactide stereocomplexes [14] demands using low cooling rates during processing in order to obtain a highly crystalline structure, which in case of the injection molding process is connected with the extension of cooling time during forming.

According to previously published studies, the annealing of PLA allows to obtain an increased crystallinity level in the post-processing procedure. The subjection of amorphous biopolyesters into elevated temperature, above the glass transition and below their melting temperature, resulting in complex relaxation [15] which may cause many beneficial changes in its properties such as an increase in hardness and scratch resistance [16], tensile strength and modulus [17] or heat resistance [18]. As reported by Yang et al., the application of annealing with properly time-temperature conditions resulted in higher glass transition (T_g) increase in comparison to modification with zinc phenyl phosphonate used as a nucleating agent [19]. The annealing procedure

* Corresponding author.

E-mail address: mateusz.barczewski@put.poznan.pl (M. Barczewski).

may also be used in more complex polymeric systems, including blends and composites. Ge et al. obtained a profitable and controlled phase separation of PLA-PBC blends, which led to the occurrence of major toughening micromechanisms [20]. Wootthikanokkhan et al. studied the effect of annealing on composites containing various fillers (montmorillonite MMT, boron nitride BN and kenaf fibers) [21]. Their results showed that incorporating particle and fibrous fillers into the amorphous PLA matrix caused hardly any effects on the heat deflection temperature, while after the annealing process, a synergistic effect of the filler addition and thermal treatment was dependent on the filler type. The most favorable effects were observed in the case of the fibrous filler, while the addition of fillers of a different origin (organic and inorganic) caused similar stiffness improvement, after annealing the composites elasticity modulus varied with the most profitable effect observed for particle-shaped fillers, i.e. MMT and BN in the PLA matrix [21]. Therefore, it can be stated that both the surface conditions, as well as the geometry of the filler, play a role in the final properties of the amorphous PLA composites subjected to thermal treatment. Detailed work of other researchers focused on the analysis of changes in the crystalline structure of PLA composites modified with inorganic particle fillers such as mica [22], calcium carbonate [23] and montmorillonite [24] showed the dominant role of polymer crystallinity on the effective strengthening of the composite at elevated temperature conditions. The synergism of the simultaneous interaction of the presence of the filler and annealing process also depended on the nucleating ability of the filler [23], however the dominant effect was assigned to post-processing conditions [24].

Due to the growing interest and demands of the industry, basalt-based fillers are gaining ground in many academic studies [25,26]. Researches focus on the modification of both thermoplastic [27,28] and thermoset [29,30] materials using basalt fibers (BF) as a replacement for glass fibers (GF) or carbon fibers (CF). The biggest advantage of BF is that their production requires hardly any additives, which makes processing them more sustainable and economically justified in comparison to GF. The main advantage of using basalt fibers in polymeric composites is the possibility of mechanical, thermomechanical and thermal properties enhancement. The subject of PLA modification using basalt fibers has been widely discussed in previously published studies [26,28,31–34]. Most of the work concerns the impact of the content of short (chopped) basalt fibers, with the length in between 400 μm and 10 mm, on the mechanical and thermomechanical properties of composites shaped in the injection process. The most beneficial effect of BF addition is a significant improvement in the mechanical properties of the composites. The incorporation of chopped basalt fibers with an average fiber length of 400 μm , allows achieving above 100 MPa tensile strength for PLA composites containing 30 wt% of BF [32]. For composites based on PLA reinforced with long basalt fibers produced by compression molding, tensile strength exceeding 300 MPa was reported [35,36], which can be comparable to glass fiber reinforced composites based on unsaturated polyester resin [37]. An additional increase in the mechanical properties of composites modified with basalt fibers has been achieved in previous practice by the introduction of modifiers or inorganic fillers such as talc, which show the nucleating ability on PLA [33,34].

In our previous studies, we investigated the possibility of applying basalt powder (BP), which is a waste product generated during the road ballast production as a filler for different polymer types [38–41]. The results clearly showed that the application of BP allows to enhance the thermomechanical and thermal properties similar to the use of basalt fibers while using significantly cheaper material.

The simultaneous effect of annealing and BF addition on PLA composites has already been described [25]. Ying et al. showed that both surface treatment, as well as the annealing procedure, have a significant effect on the mechanical properties of composites reinforced with chopped basalt fibers with a length of 5 mm. Their results showed a similar effect of a 20% increase in tensile strength improvement connected with the application of both silane surface modification and

annealing.

Our studies were undertaken with the aim of minimizing the potential production costs of the finished biodegradable products. We compared the effectiveness of the particle and fibrous basalt-fillers with the simultaneous use of the annealing procedure on the thermo-mechanical properties of the PLA matrix. Moreover, in comparison to the studies already described in the literature, we used unchopped micrometric basalt fibers (BMF) with a length of up to 150 μm , obtained by the milling process, rather than short fibers. The use of the fillers, as well as the post-processing method, was based on two assumptions: that the basalt fibers could be replaced by low-cost waste basalt powder and that the thermal treatment may be used as a cost-effective way to improve the performance of biopolyesters and their composites which may exclude the necessity of using nucleating agents and limitations resulting from affecting the processing cycle time realized in order to improve the crystallinity of PLA. The main purpose of the PLA-BP/BMF materials presented in this study is to become the matrix for the production of the long fiber-reinforced composites, with the assumption of two-step processing, including compression or injection molding by insert overmolding technique. Undertaken modification procedure is focused on the possibility of thermomechanical stability improvement with the simultaneous reduction of the polymeric content in the composite without a strong deterioration of the mechanical properties.

2. Experimental

2.1. Materials and sample preparation

Commercial grade polylactide (PLA) Ingeo™ 2500HP, with a melt flow rate (MFR) of 8 g/10 min (210 °C, 2.16 kg), density of 1.24 g/cm³, D-Lactide content of 0.25 mol%, molecular weight $M_n = 71,900$ Da and dispersity $D = 1.62$ [42,43] supplied by Nature Works (USA) was used.

Two types of basalt fillers were used in this study: basalt powder (BP) and micrometric basalt fibers (BMF). The natural basalt powder (BP), which was a waste product from the production of track ballast rocks, was mined in Wilkow (Poland). The inorganic particle-shaped filler was characterized by the average particle size of 10.2 μm and moisture content, determined with TGA as a mass loss at 130 °C of 1.6%. The dominant chemical ingredients of BP were as follows: SiO₂ (49.5%), Al₂O₃, (15%), CaO (9.6%), FeO (8.7%), MgO (6.8%) and Fe₂O₃ (3.7%) [44]. Micrometric basalt fiber (BMF) MICF0021 manufactured by the milling process was purchased from Incotology (Germany), and was produced without any sizing and chemical surface treatment. The fiber-shaped filler was characterized with 8–13 μm diameter, 5–150 μm length, 2.65–2.75 g/cm³ density, and moisture content of 1.2%, determined with TGA as a mass loss at 130 °C. BMF have the following chemical structure: SiO₂ (41–55%), Al₂O₃ (10–20%), FeO/Fe₂O₃ (7–18%), CaO (6–13%), MgO (1–15%), Na₂O (2–7.5%) and TiO₂ (0.5–3%) [45].

Prior to the mixing process, PLA pellets were ground into a powder after cooling with liquid nitrogen. The irregularly shaped PLA powder was mechanically mixed with 5, 10 and 20 wt% of the filler respectively and dried using Memmert ULE 500 dryer at 70 °C for 24 h. Next, all the materials were mixed in a molten state by means of a ZAMAK EH-16.2D twin-screw co-rotating extruder. The processing was realized at the maximum temperature of 190 °C and rotational speed of the screws 100 rpm, and pelletized after cooling in forced airflow. Specimens with dimensions according to ISO 527 were formed using a Battenfeld PLUS 35 hydraulic injection molding machine operating at the maximum processing temperature of 210 °C. The injection molding process was conducted under the following conditions: mold temperature 50 °C, injection speed 75 mm/s, forming pressure 72 MPa and cooling time 50 s. After forming and conditioning for 7 days, selected samples were annealed in Teflon molds in order to cause the recrystallization process. Annealing was realized in Memmert ULE 500 laboratory dryer for 3 h and an elevated temperature of 100 °C. The annealing temperature was

based on preliminary DMA experiments, taking into account the literature data. The temperature of 100 °C allowed to obtain a combination of two different PLA crystalline forms α and α' , due to being in the middle of the transition region (85 °C and 145 °C for α and α' respectively) [46, 47]. The samples were described in reference to the amount and type of the filler as PLA; 5BP; 10BP; 20BP; 5BMF; 10BMF; 20BMF. Series of the samples subjected to the annealing process were assigned with additional “-a” suffix, e.g., PLAA, 10BPa.

3. Methods

Differential scanning calorimetry (DSC) measurements were performed using a Netzsch DSC 204 F1 Phoenix® apparatus with aluminum crucibles and approximately 5 mg samples under nitrogen flow. All the samples were heated up to 210 °C and held in a molten state for 5 min, followed by cooling down to 20 °C. Heating and cooling rates were equal to 10 °C/min. This procedure was conducted twice to evaluate the DSC curves from the second melting procedure and gain extensive information about the influence of both the nucleating ability of basalt fillers as well as processing and post-processing of PLA and its composites. The crystallinity degree X_C was calculated according to the following formula (1):

$$X_C = \frac{\Delta H_M - \Delta H_{CC}}{(1 - \phi) \cdot \Delta H_{100\%PLA}} \cdot 100\% \quad (1)$$

where: ΔH_M is the melting enthalpy of a sample, ΔH_{CC} is the cold crystallization enthalpy of a sample, $\Delta H_{100\%PLA}$ is the melting enthalpy of the 100% crystalline PLA, $\Delta H_{100\%PLA} = 93$ J/g [48], ϕ is the filler content.

The influence of BP and BMF on the changes in the crystalline structure of PLA was investigated with polarized light microscopy (POM) using a Nikon polarizing light microscope equipped with a Linkam TMHS 600 hot stage. The 15 μ m thick microtome cut samples were squeezed between two microscope glass slides, then inserted in the hot stage. The evaluation of the growing spherulite structure was monitored during solidification by taking photomicrographs at appropriate intervals of time, using an Opta-Tech digital camera. The analysis was conducted with the magnification of 200 \times . In order to obtain extensive information about the influence of basalt fillers on the structure of PLA-BP/BMF composites, solidification from the molten state was conducted under non-isothermal and isothermal conditions. In the case of the non-isothermal experiment, each sample was heated from 25 to 210 °C at a rate of 10 °C/min, melted at 210 °C for 5 min to erase previous thermal history, and cooled down to 20 °C with the cooling rate of 10 °C/min. In the case of isothermal test, after melting, the samples were cooled to 130 °C with a cooling rate of 5 °C/min, and maintained at this temperature for 30 min.

Linear shrinkage of the PLA and its composites was evaluated by measurements of sample length formed in the injection molding cavity characterized with 4.15 \times 10.15 \times 121.2 mm³ dimensions using a Mitutoyo electronic caliper. Each evaluation was based on measurements of 15 specimens.

The structural changes evaluation caused by the incorporation of the filler was determined by scanning electron microscopy (SEM). The samples' fracture surfaces were examined and digitally captured using a scanning electron microscope Tescan VEGA 5135 MM. The electron accelerating voltage of 12 kV was applied. The samples were fractured after being cooled in liquid nitrogen, in order to reduce the effect of plastic deformation influencing the polymer-filler interface. Prior to the tests, all the specimens were sputtered with a layer of gold. The magnifications of 2000 \times and 5000 \times were used.

Heat deflection temperature (HDT) investigations were conducted with the use of the CEAST HV3 apparatus. The measurements were carried out in an oil bath in accordance with ISO 75 standard HDT B type experiment was prepared with a heating rate of 120 °C/h and stress 0.45

MPa.

The dynamic mechanical properties of the composites, with 10 \times 4 \times 50 mm³ dimensions, were studied using DMA methods in a torsion mode, operating at the frequency of 1 Hz and strain of 0.01% in the temperature range between 25 °C and 100 °C, and at the heating rate of 2 °C/min.

The mechanic properties of pure PLA and PLA-BP/BMF composites were evaluated in a tensile test according to ISO527 standard by means of Zwick Roell Z020 universal testing machine with 10 kN force sensor. The tests were carried out with a crosshead speed of 1 mm/min during the determination of elasticity modulus and 50 mm/min during the determination of tensile strength and elongation at break. Each evaluation was prepared for 15 test specimens.

The impact strengths of the unnotched samples with 10 \times 4 \times 15 mm³ dimensions were measured by the Dynstat method using a Dys-e 8421 apparatus equipped with a 0.98 J hammer according to the DIN 53435 standard. The presented impact strength values are the arithmetic means calculated from 15 measurements.

Brittleness was calculated by means of the procedure described by Brostow et al. [49] according to the following formula (2):

$$B = \frac{1}{(\epsilon_b \cdot E')} \quad (2)$$

where: ϵ_b is the elongation at break determined in tensile test measurements, and E' is the storage modulus determined by dynamic mechanical analysis (DMA) at a defined temperature and 1 Hz frequency. In this study, the values of storage modulus (G') determined in a torsion mode of DMA analysis were applied to Equation (2).

4. Results and discussion

4.1. Thermal properties

Fig. 1 shows the first and second heating curves of PLA and PLA-BP/BMF composites obtained during the DSC experiments, while the thermal properties, including crystallinity (X_c) calculated according to formula (1), melting (T_m) and crystallization (T_c) temperatures are presented in Table 1. It can be seen that the nucleating ability of both fillers was insufficient to obtain the dominant semicrystalline structure of the PLA-based composites in the rapid cooling conditions during injection molding. The cold crystallization effect may be observed for all first heating curves, however the cold crystallization phenomenon occurred during the second heating only in the case of the unmodified PLA sample. The lack of the exothermic peak in the range of up to 110 °C for composite samples suggests a limited nucleating ability of both basalt derivatives. The slow cooling rate (10 °C/min) during the cooling in DSC chamber from the melt in the controlled thermal conditions was sufficient to obtain crystallization from the melt of the filled PLA. The small exothermic peak near 160 °C observed for all the samples during heating independently of thermal treatment suggests the α' to α transition of PLA [47]. This suggests also that using basalt powder and fibers did not provoke polymorphic changes during the crystallization of PLA. The crystallization temperature values confirm a slightly higher nucleating ability of the BP. The crystallization temperature of both composite types was almost independent of the filler content. The addition of a higher amount of BP and BMF resulted only in about 1 °C improvement of T_c in comparison to the composites with the lowest filler content. The significant difference between the crystallinity level of PLA and its composites determined on the basis of the first and second heating was observed. After being formed in rapid cooling conditions during the injection molding process, all the samples showed an amorphous structure and comparable crystallinity level ca. 18%. The application of a controlled cooling rate during the DSC experiment (after erasing the thermal history of the samples) shows a nucleating behavior of both basalt derivatives. The results are in good agreement with crystallization

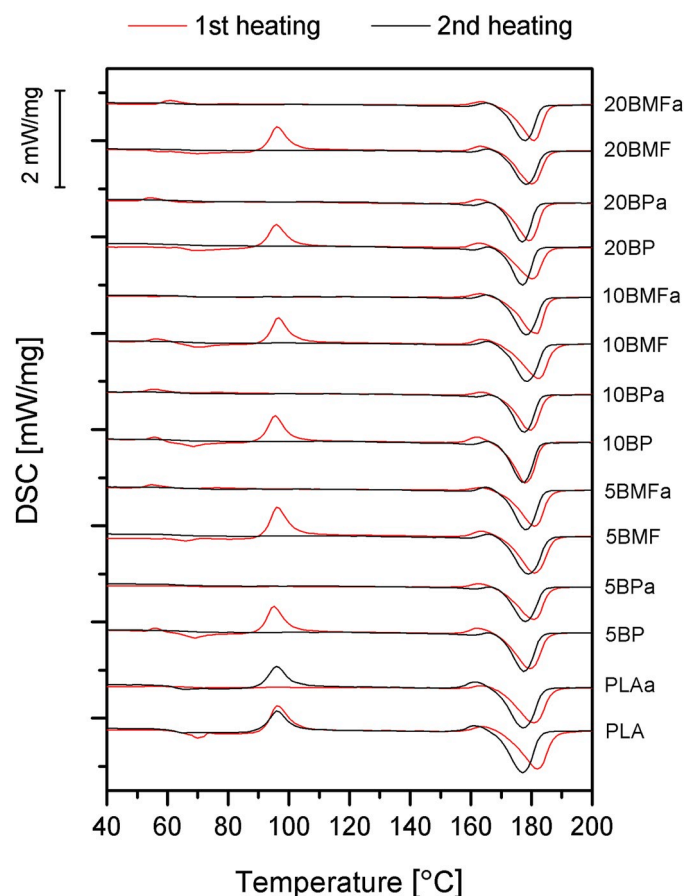


Fig. 1. DSC 1st and 2nd heating curves of PLA and PLA-BP/BMF composites.

Table 1
Thermal properties of PLA-BP/BMF composites obtained by DSC.

Material	T _c [°C]	T _m 1st heating	T _m 2nd heating	X _c 1st heating [%]	X _c 2nd heating
PLA	95.3	181.9	177.1	18.1	22.4
5BP	103.5	181.0	177.5	16.5	45.8
10BP	103.1	177.8	177.1	18.5	47.2
20BP	103.9	180.4	176.9	16	49.7
5BMF	101.1	179.7	178.9	16.6	47.5
10BMF	101.0	182.3	178.5	18.1	45.2
20BMF	101.8	181.1	177.9	16	45.8
PLAa	96.1	180.9	177.2	45	–
5BP _a	103.2	180.8	177.9	41	–
10BP _a	103.4	179.4	177.5	44.1	–
20BP _a	103.9	179.4	176.9	49.3	–
5BMF _a	101.6	181.0	178.2	43.8	–
10BMF _a	101.6	181.8	178.3	43.2	–
20BMF _a	102.0	180.8	177.7	46.1	–

temperature values, i.e. higher crystallinity was observed for composites filled with the particle-shaped filler. In the case of annealed samples, all the materials revealed a similar level of crystallinity, which suggests the dominant role of cold crystallization. A similar effect of the negligible effect of organo-modified montmorillonite content on the crystallinity of PLA based composites subjected to annealing was reported by Picard et al. [24]. 20BP_a sample shows a similar level of crystallinity to 20BP during the second heating; this phenomenon may be a result of the synergistic effect of the nucleating ability of BP and annealing. No difference in X_c of 20BP and 20BP_a samples confirms that the application of only BP may be sufficient to obtain a high crystallinity level in the case of low cooling rate application.

4.2. Structure evaluation

Fig. 2 shows the structures of PLA and PLA-BP/BMF composites filled with 5 wt% of the inorganic particles and fibers obtained during non-isothermal (2 a-c) and isothermal (2 c-d) crystallization. The results obtained by both experiments showed a similar effect of lowered spherulite size for the composite containing BP, more distinct after isothermal crystallization. The composites containing BP were also characterized by a more uniform size and distribution of crystalline domains in the evaluated space, which suggests a higher nucleating ability of the particle-shaped filler. In the lower right corner of the microphotography obtained for the 5BP sample crystallized under isothermal conditions, a small transcristalline layer (TCL) around the basalt particle with a size of about 40 μm can be observed. Interestingly, no transcristalline region around BMF was observed, which indicates that this filler reveals a weak nucleating ability on PLA. A similar effect of no TCL was also observed for PLLA filled with flax fibers by Wong and coworkers [50]. On the contrary, Liu et al. reported the nucleating ability of BF on PLA with the formation of the transcristalline region in the interface after isothermal crystallization conducted at 120 °C [51]. The difference may be an effect of the lack of silane treatment of BMF used in our study. The formation of the transcristalline phase is strongly dependent on the molecular weight and stereoregularity of PLLA [52]. The higher amount of the spherulites with lowered size in the case of the PLA-BP composite may be a result of the creation of TCL around the irregularly-shaped particles with a higher free surface. It cannot be neglected that the higher ability to create a crystalline structure in the case of both composite types resulted from low-scale hydrolytic degradation effects occurring during the melt processing induced by residual moisture contained in the filler (higher in the case of BP).

Fig. 3 summarizes the values of linear shrinkage measured for PLA and its composites before and after the annealing process. Usually, the addition of inorganic fillers reduces the shrinkage effect of thermoplastic polymers [53]. In the present case, injection-molded samples containing BMF were characterized by an increased effect of the filler on shrinkage reduction, which is due to its higher aspect ratio and flow orientation [54]. The annealing process caused a notable change of specimens' linear dimensions. The obtained shrinkage values of the untreated PLA and PLA-BP/BMF composites are relatively small and consistent with the literature data obtained for PLA formed at comparable mold temperature [55]. It should be mentioned that post-mold annealing can increase the final shrinkage of injection molded parts, and it is usually the higher, the lower mold temperature during forming [54]. The long holding time of 25 s and application of low mold temperature (50 °C) allows obtaining injection molding samples with low crystallinity and low shrinkage values [56]. However, the residual stresses formed during injection molding due to the quenched oriented structure of amorphous PLA were subjected to relaxation during thermal treatment, which resulted in linear shrinkage of specimens [57]. The significant change of the PLA crystallinity, as well as its relatively low value before annealing, additionally led to increasing of linear shrinkage after recrystallization. This phenomenon may be limited in case of higher X_c values before thermal treatment. Barletta and Puopolo, in their study [58] showed a negligible effect of annealing process on shrinkage of injection molded thin-walled PLA products. However, the difference of the crystallinity change induced by thermal treatment was twice lower than the achieved in this study as well as the initial value of X_c was twice higher.

The influence of annealing on the structure of PLA, 20BP and 20BMF samples was analyzed using SEM. Fig. 4 shows the images of fractured surfaces of the mentioned samples. It can be seen that annealing results in a change in the nature of the fracture. The annealed samples showed a more developed structure without large brittle cracks such as those observed for the untreated samples, which is typical for semicrystalline polymers and the occurrence of plastic deformation. Although several pull out holes were observed in the image of 20BP_a, most of the inorganic particles are well saturated by the PLA matrix. Particle distribution

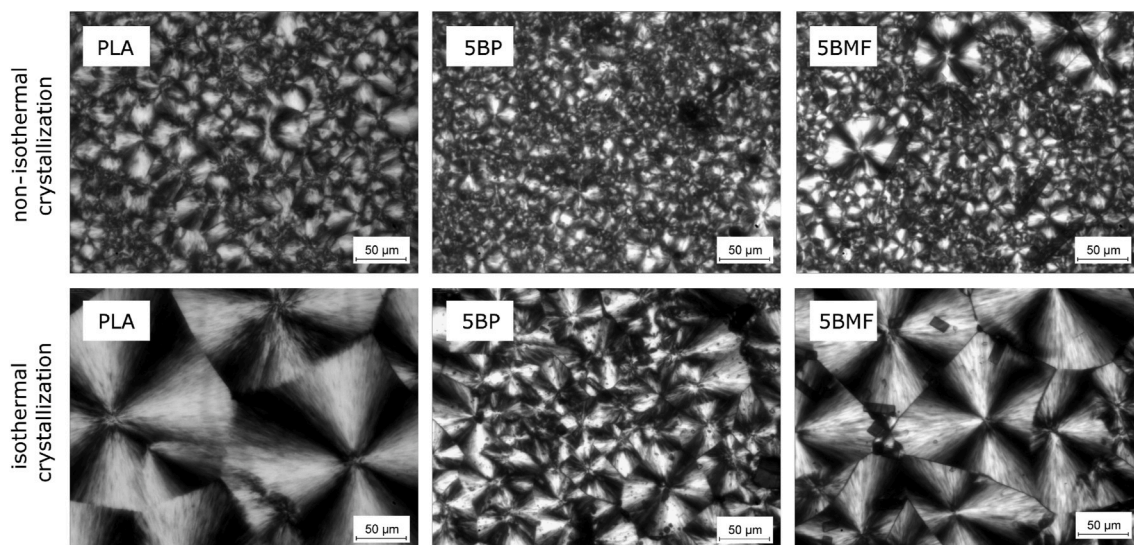


Fig. 2. Polarized optical microscopy images of PLA, 5BP, 5BMF obtained under non-isothermal and isothermal crystallization.

in the composite may also be described as uniform. A more distinct effect of annealing may be observed for samples containing 20 wt% of the micrometric basalt fiber (an additional SEM image made with higher magnification, Fig. 5). While properly realized annealing process usually causes the improvement of the bonding at PLA-filler interface [22], in selected cases may also result in weakening of the interfacial adhesion [59]. It can be clearly seen that after annealing and the cold crystallization process of PLA corresponding to this procedure, the adhesion between the polymeric matrix and basalt particles and microfibers was lost. Both distinct gaps in the interfacial region and pull out holes are visible around the BP and BMF particles. On the other hand, in the

untreated 20BMF sample SEM image fibers are well covered with the polymer without any adhesion failures, and breakage of the fibers occurred at the plane of the fracture. The main difference between the two filler types is caused by the different shapes of the filler. BP is characterized by a low aspect ratio and a more developed free surface, which allows obtaining better saturation of the filler by molten polymer than in the case of BMF. The interfacial adhesion between PLA and filler is the simultaneous effect of better compatibility and formation of the transcrystalline region induced by chemical treatment of the filler [60]. The BP showed better nucleating ability and creation of transcrystalline region at the surface in contrast to BMF. Due to the higher aspect ratio of

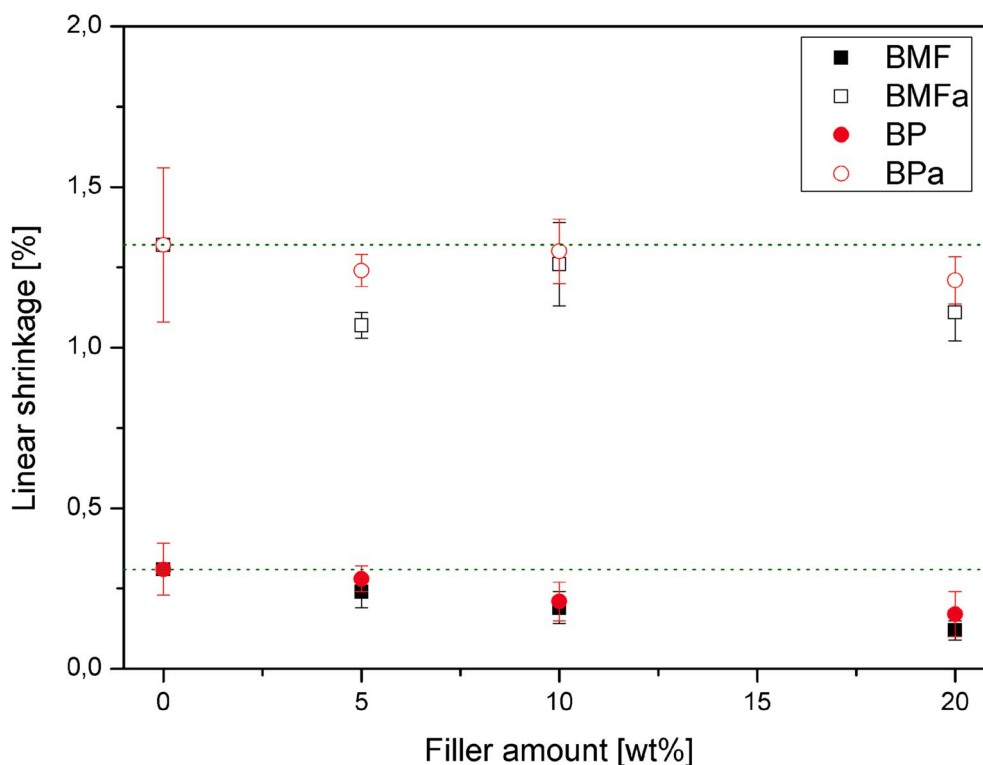


Fig. 3. Linear shrinkage of PLA-BP/BMF composites subjected to the annealing process.

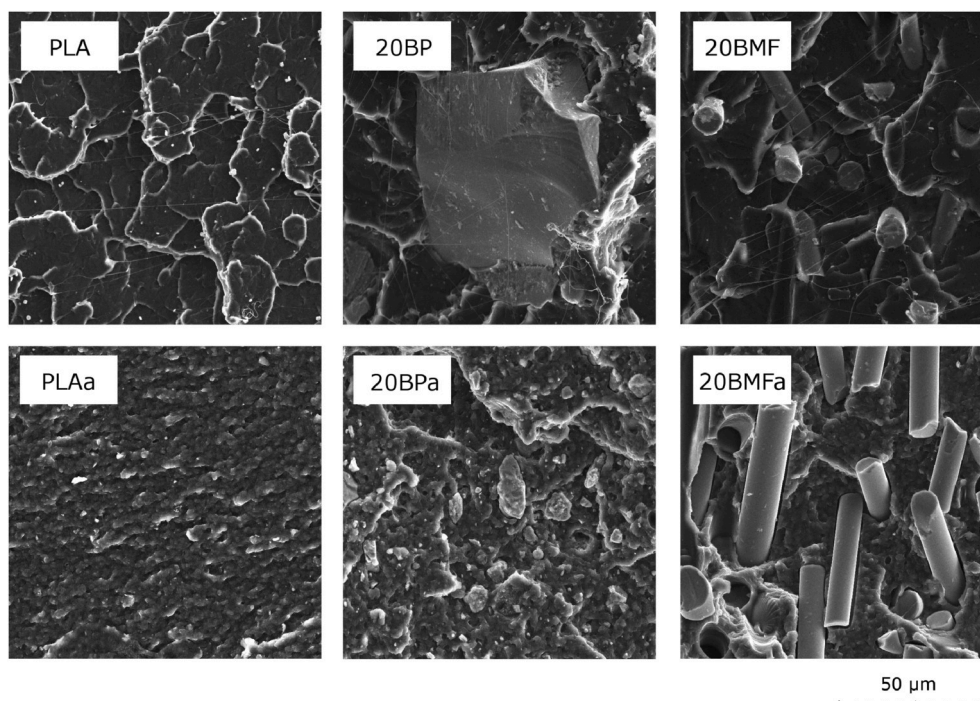


Fig. 4. SEM image of PLA and PLA-composites containing 20 wt% of the filler before and after annealing.

the BMF and more regular shape, the difference between thermal dilatation of the inorganic filler and PLA during cold crystallization was more distinct and resulted in the higher loss of the adhesion in the interfacial region.

4.3. Thermomechanical properties

Fig. 6 shows the results of heat deflection temperature measurements. As can be seen, the addition of both filler types into PLA in the amorphous state did not influence the thermomechanical stability of the composites. The annealing process resulted in a 27% increase in the crystallinity of PLAA, which caused a 100% increase in the HDT value in reference to the untreated PLA. The incorporation of both basalt fillers caused an additional increase in HDT. The amount of the filler, which effectively improved the thermomechanical stability, was 10 wt% and 20 wt% for BP and BMF, respectively. The synergistic effect of PLA double modification, including annealing and addition of basalt derivatives, allowed to obtain 13 °C (BP) and 15 °C (BMF) increase in HDT in reference to the PLAA samples (119 °C).

The thermomechanical behavior in dynamic mechanical strain conditions was determined using DMA. Fig. 7 shows the influence of the addition of the two basalt derivatives and annealing on the run of storage modulus (G') and damping factor ($\tan\delta$) vs. temperature (T) curves. For both composite types that contained fiber- and particle-shaped fillers, the storage modulus curves show a course typical for amorphous PLA with a significant drop in stiffness in the range of the amorphous phase relaxation, which according to the DSC data was dominant in the structure of the polymeric matrix. The addition of both basalt derivatives, especially in the case of the highest content of the filler, caused an increase in storage modulus in the whole considered temperature range. This phenomenon resulted rather from the effect of the sufficient filler content than its nucleating ability, because – as it was proved – the untreated PLA-BP/BMF composites crystallinity was independent of the filler content. However, the presence of inorganic fillers shifts the increase in the G' caused by cold crystallization to higher temperature values, which suggests a higher level of macromolecular arrangement during cooling. All the samples subjected to annealing

showed no abrupt drop in the stiffness at the beginning of the glass transition nor cold crystallization, which is mainly related to the reduced amount of the amorphous domains [61]. Additionally, unlike for the untreated composites, increased stiffness of the annealed composites corresponded to the content of the filler. A similar effect was observed for PLA-talc composites subjected to annealing by Battagazzore et al. [62], however in the case of the application of talc as a filler with the lowest Mohs hardness this change was attributed to its nucleating ability rather than its reinforcing effect. It can be stated that stiffness improvement measured as HDT as well as DMA (G') was a synergistic effect of recrystallization and the presence of rigid inorganic domains of the basalt fillers. However, the reinforcing effect of inorganic fillers dispersed in the PLA matrix is straightly connected with high storage modulus at elevated temperature resulting from the crystalline structure of the matrix [22].

The damping factor ($\tan\delta$) values presented as a function of temperature in Fig. 7 were one order of magnitude lower for the annealed composites. This effect is related to the rearrangement of the amorphous structures of polylactide during thermal treatment, and increased stiffness of the composites at elevated temperature. The additional reduction of $\tan\delta$ value at the glass transition region caused by the presence of the inorganic fillers as an effect of their reinforcing efficiency was also reported for PLA-based composites subjected to annealing filled with talc [62] and bamboo fibers [63]. It should be stressed that a different tendency in the glass transition temperature peak shift caused by the presence of the filler was observed for the untreated and annealed samples. In the case of the composites which were not subjected to thermal treatment, a slight shift in the glass transition was observed for the samples with the highest amount of the filler after processing, whereas the annealed samples show the opposite tendency. This phenomenon may be related to the loosened adhesion in the interface between the polymer and the filler [64], which is in good agreement with the SEM analysis.

The synergistic effect of both modification methods was also confirmed by the analysis “C” factor, which allows assessing the effectiveness of the filler on the polymeric matrix in a quantitative way. The values of “C” factor can be calculated according to the following formula

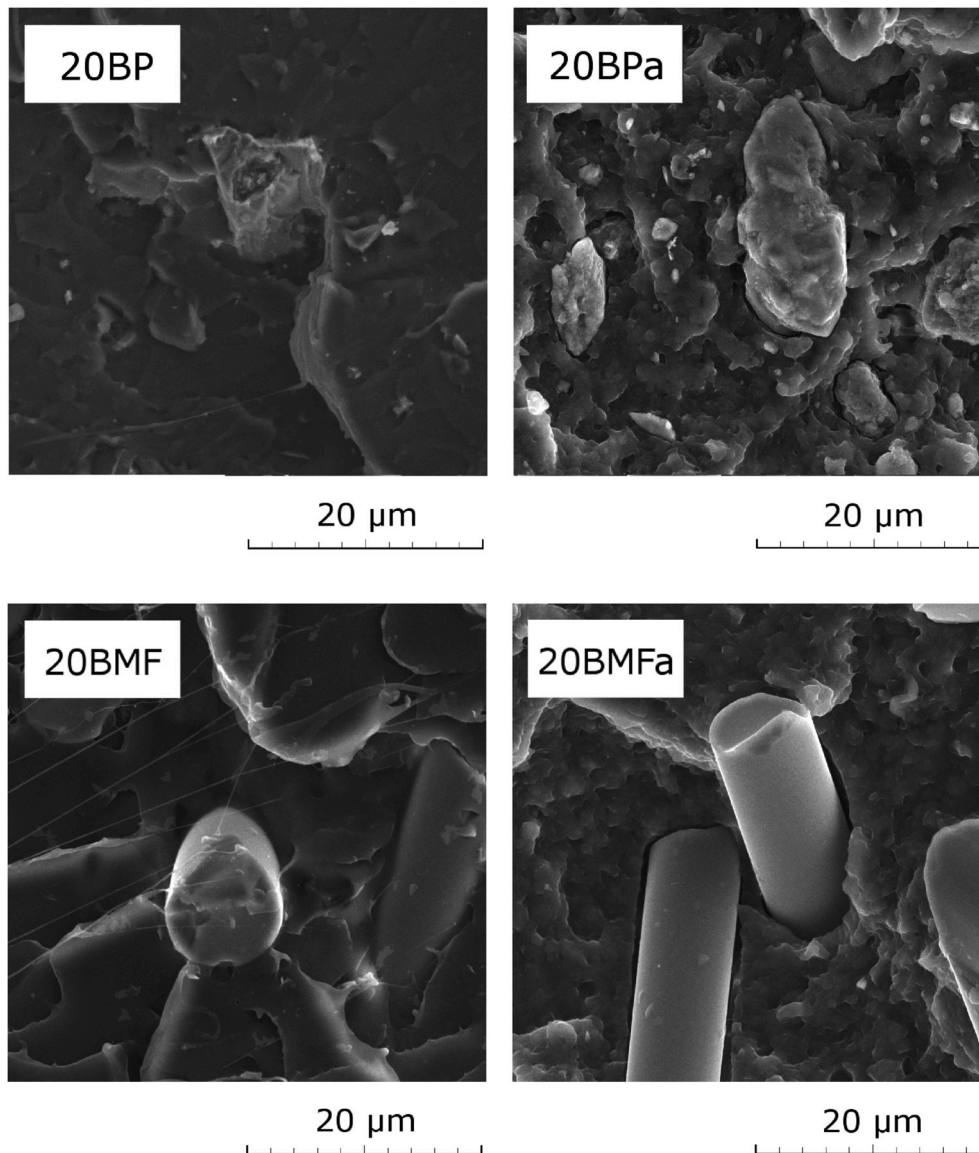


Fig. 5. SEM image of an interfacial region of composites containing 20 wt% of BP and BMF.

(3):

$$C = \frac{(G'_g / G'_r)_{\text{composite}}}{(G'_g / G'_r)_{\text{matrix}}} \quad (3)$$

where G'_g and G'_r are the values of storage modulus determined in the glassy state and in the rubbery state, after passing the glass transition of the material.

The values of C factor are presented in Table 2. The effectiveness of the filler calculated in reference to pure PLA for the untreated samples shows relatively high values, which indicates poor effectiveness of the filler. The difference between the effect of the two fillers on the stiffness of the samples in the considered temperature values is clearly visible. For BP-filled PLA composites, no distinct tendency was observed, while increasing the content of BMF resulted in the gradual lowering of the C value. The effectiveness of the filler for the composites with the amorphous PLA matrix filled with the particle-shaped filler was independent of the filler content, which suggests the dominant role of the nucleating ability of BP over the reinforcing effects caused by the presence of rigid basalt structures. For the annealed samples, the C factor values show a distinct tendency to increase the efficiency of the filler on the

thermomechanical properties modification dependent on the filler content. For the thermally treated samples, the thermomechanical parameter was calculated in reference to the annealed pure PLA as well as the untreated sample (results indexed with *). The C factor values calculated in reference to the untreated PLA are low, which may be interpreted as a significant improvement of the thermomechanical stability of the composites. For the composites with the PLA matrix containing a higher amount of the crystalline phase efficiency of the filler was slightly higher for BMF.

4.4. Mechanical properties

Fig. 8 shows the mean values of selected mechanical parameters obtained by a tensile test, impact strength measurements and a hardness evaluation. The results of a tensile test proved that the annealing process has a major influence on mechanical properties. Despite the fact that the addition of both basalt derivatives caused increasing stiffness of the composite samples, 17% improvement of elasticity modulus was observed only for the samples with the highest content of BMF. Tensile strength was reduced by the addition of the basalt fillers. While for BP this effect is reasonable and it is typical for particle-shaped inorganic

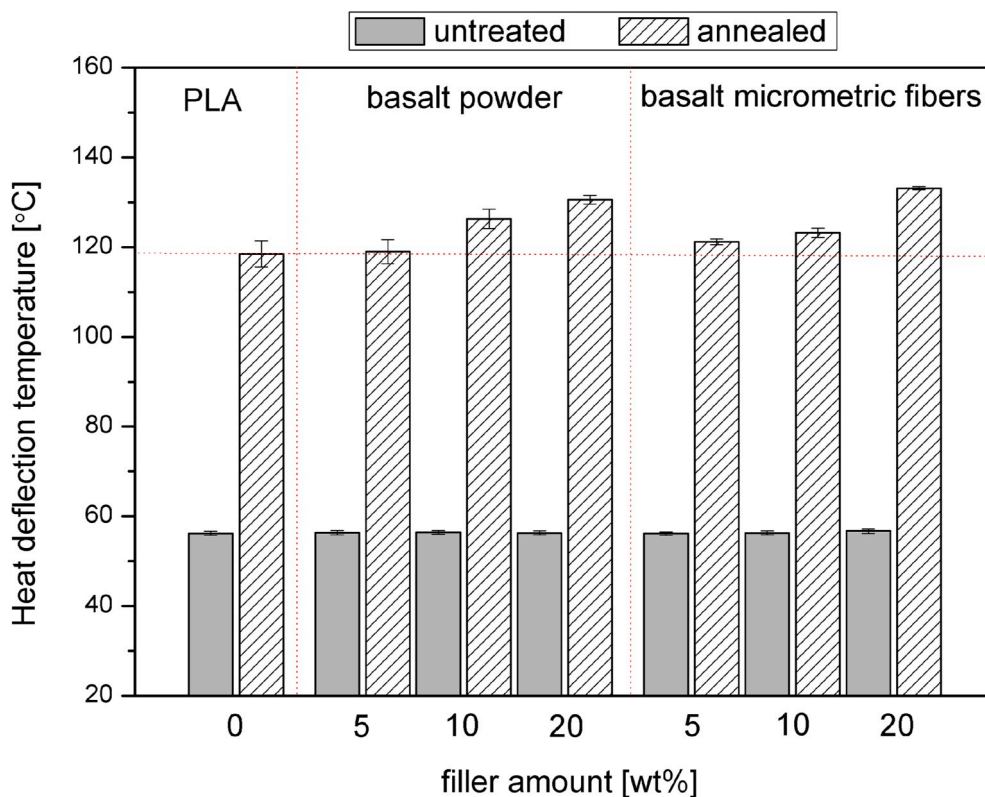


Fig. 6. HDT values of PLA and PLA-BP/BMF composites.

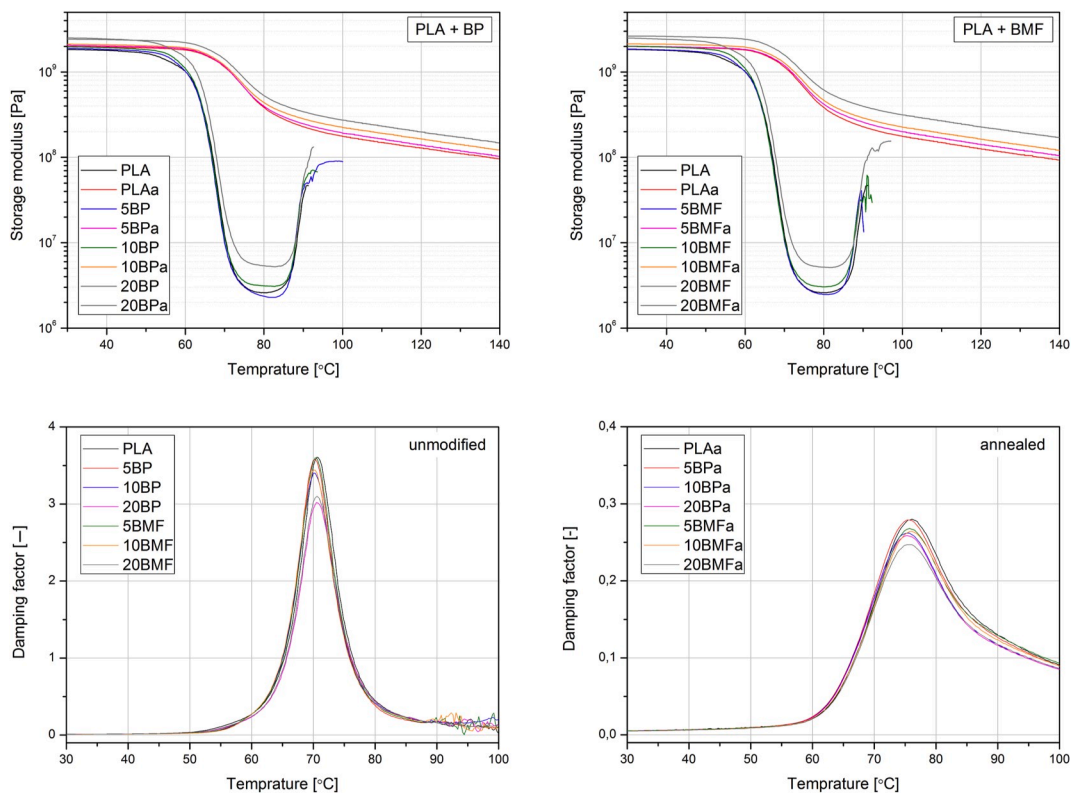


Fig. 7. G' and $\tan\delta$ vs. temperature curves obtained by DMA.

Table 2
Effectiveness of the filler calculated C factor based on DMA data.

Material	C [-]		
	untreated	annealed	
PLA	-	-	0.0074*
5BP	0.599	0.991	0.0073*
10BP	0.897	0.921	0.0068*
20BP	0.660	0.875	0.0065*
5BMF	1.065	0.913	0.0068*
10BMF	0.931	0.876	0.0065*
20BMF	0.683	0.816	0.0061*

*C calculations referred to untreated PLA.

filler due to low aspect ratio and the presence of the areas of imperfect adhesion at the developed surface of the filler which causes stress concentration [65], the reduction of the tensile strength of the BMF-filled composites may be directly related to insufficient adhesive bonding between PLA and BMF. A similar effect was described by Tábi et al. for

PLA-based composites filled with untreated BF [26]. It should be stressed that no significant effect of the thermal treatment was observed for any sample, nor any reduction in mechanical resistance determined in a static test showed to be significant enough to exclude either composite type for application as construction materials. PLA showed a 200% increase in elongation at break in comparison to the untreated pure PLA sample after the recrystallization of the polymeric structure caused by annealing. All BP-filled and untreated BMF-filled composites showed elongation values comparable to the one of the amorphous PLA. A different behavior was noted for the annealed composites containing BMF. In reference to the SEM analysis and DMA measurements, it can be stated that increased elongation at break of the BMFa composite series resulted from a drastic failure of the adhesion between the filler and the polymeric matrix. Adhesion loss caused the transfer of all strain by the matrix; only in the case of the 20BMFa sample elongation at break was lowered in comparison to the PLAa.

The thermal post-processing procedure used for the modification of PLA and its composites plays a dominant role in the hardness changes

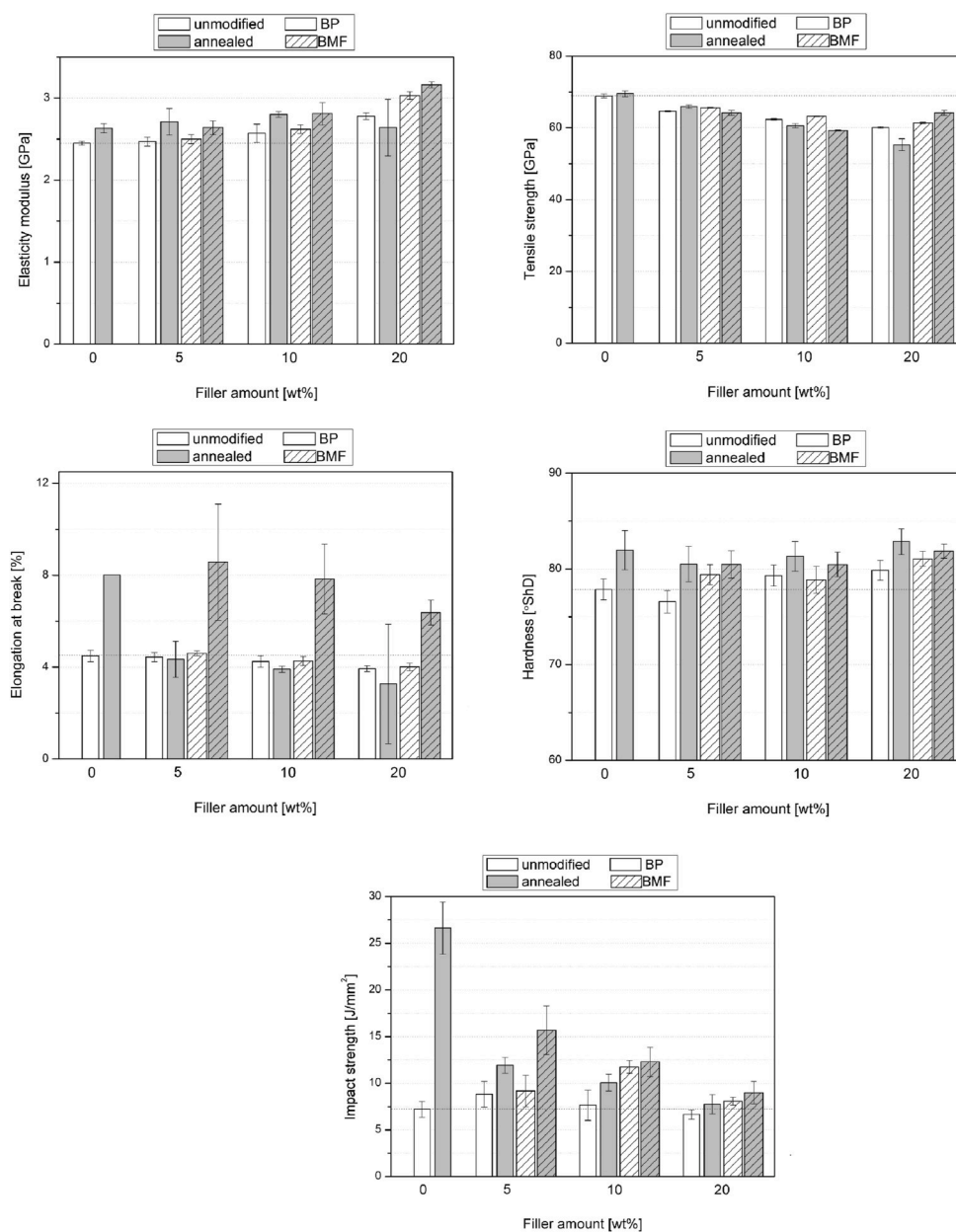


Fig. 8. Results of mechanical properties evaluation.

presented in Fig. 8. The additional presence of both fillers resulted in no visible change of the hardness in comparison to the PLAA. The crystallinity increase caused by annealing, as well as the presence of inorganic fillers, caused about 5°ShD improvement of this mechanical parameter. A similar dependence between increased crystallinity and hardness was previously described by Yi et al. [16].

Usually incorporating inorganic fillers results in a significant decrease in impact strength, because dispersed particles or fillers act as notches and become active centers of fracture initiation [66]. For the considered materials, the tendency for changes in the properties of the materials is opposite, which results from complex modifying effects of the BP and BMF on the PLA matrix. The annealing of PLA increased impact strength from 7.5 to 26 J/mm². Moreover, the addition of the basalt fillers allowed to reduce the brittleness of PLA, which may be correlated with the nucleating ability of BP and BMF. As it was presented, the composites containing basalt derivatives subjected to annealing showed higher crystallinity than untreated samples, which beneficially influence the resistance to impact load. Even the composites with the highest filler content showed impact strength comparable to the one of the unmodified PLA sample. The highest impact strength values of all the composite samples were measured for the BMFA composites. This phenomenon is probably a result of the lack of proper adhesion between the matrix and filler and the negligible role of the fibrous filler in strain transfer during impact load rather than the high crystallinity of BMF-filled composites. It can be supposed that the composites after annealing with loosed adhesion between the polymer and filler behave as a polymer with non-regular microcellular structure, which, as it was reported in some cases, may reveal improved impact properties [67,68]. Therefore, the higher impact strength of the composite samples subjected to annealing may be a simultaneous effect of improved crystallinity achieved for filled materials, and the 'pseudo-porous' structure occurred by the significant loss of the polymer-filler interfacial bonding. The reduction of the beneficial changes in the ductility of the semi-crystalline PLA caused by the increased amount of the two fillers is connected with the yields plastic deformation around the particles or fibers near the notch reducing the micro void concentration, which became dominant in the fracture behavior over PLAA improved ductility caused by the rearrangement of the amorphous domains [69].

Multicriterial brittleness parameter calculated according to Brostow [49] allows to qualitatively describe the influence of different structural effects occurring in both unfilled polymers as well as composite materials [70,71]. The values of brittleness presented in Table 3, determined in ambient temperature, suggest that the composites with the PLA matrix in the amorphous state show a similar modification effect. The low nucleating ability of the basalt derivatives resulted in a higher crystallinity of composites, which compensate for potentially increased brittleness resulting from the presence of the stiff domain of the fillers. Therefore lowered B values were observed for the untreated composites containing 20 wt% of BP/BMF. After annealing the PLAA sample exhibited brittleness reduced almost by a half in reference to the untreated PLA due to a significant increase in crystallinity. The annealing of the composite materials provided different effects. All the BP-filled

composites showed similar brittleness, at the level comparable to the non-annealed samples. However, for the fibrous filler the application of double modification (annealing and BMF incorporation) caused a significant drop of brittleness. The calculated values were even lower than those obtained for the PLAA. As mentioned at the beginning of this section, the evaluation of B factor may be a useful tool for determining structural changes in materials. Unfortunately, in the presented case, the lowered brittleness was not a beneficial effect of BMF and annealing but rather a result of adhesion failure in the polymer-filler interfacial region in the form of debonding, as it can be observed in the SEM image (Fig. 5). During annealing resulting in the reorganization of the macromolecular structure of the polymeric matrix, there occurred relatively high shrinkage of injection molded samples. The adhesion between PLA and BP/BMF was loosened as an effect of different thermal expansion of both composite ingredients. This phenomenon was more distinct in the case of the BMF-filled composites, probably due to the higher aspect ratio of the fibers and less developed structure of the filler with a lower ability to saturation by a polymer. As can be seen, the Brostow brittleness factor may be useful not only to verify the modification effects but also to describe structural defects occurring indirectly in the composite material.

5. Conclusions

The synergistic effect of the addition of two different basalt fillers (micrometric basalt fiber and basalt powder) and annealing on thermomechanical, mechanical and structural properties of PLA has been investigated and discussed in detail. It was found that both composite series formed with rapid cooling conditions showed an amorphous structure, similarly to the unfilled PLA. Even though the adhesion of the filler and the matrix evaluated by SEM was sufficient and an increase of elasticity modulus was observed (especially for the composites filled with BMF), the influence of the basalt fillers on thermomechanical stability of the samples was negligible. The application of heat treatment induced the most beneficial change in the material's properties. Annealing in 100 °C for 3 h resulted in a notable growth of the polymer's crystallinity, and consequently – the increase of heat deflection temperatures. This procedure caused an increase of HDT for the pure PLA to 119 °C, the addition of 20 wt% of BP and BMF resulted in an additional increase of 14 °C. Therefore, the efficiency of the double-modification procedure, including the application of basalt derivatives and thermal post-processing results from both an increase in PLA crystallinity as well as reinforcing efficiency of rigid BP/BMF structures. What's more, it was found that the nucleation efficiency of the two untreated basalt fillers was different. Due to differences in particle geometry, the basalt powder showed a more profound influence on PLA crystallization than the fiber-like filler, which resulted in the creation of a transcrystalline layer and improvement of filler-polymer interactions. On the contrary, micrometric basalt fiber was showed to lose the adhesion to PLA due to annealing because of higher aspect ratio, lower saturation with the polymer and differences in thermal expansion coefficient. As the influence of both filler types on the thermomechanical performance of PLA-based composites was comparable, it can be concluded that choosing sustainable, cost-effective basalt powder over basalt micrometric fiber can be highly beneficial in selected applications.

Declaration of competing interest

The authors declare that they have no known competing financial interests or personal relationships that could have appeared to influence the work reported in this paper.

CRedit authorship contribution statement

Mateusz Barczewski: Conceptualization, Project administration, Funding acquisition, Supervision, Methodology, Writing - original draft,

Table 3
Brittleness B of PLA and PLA-BP/BMF composites before and after annealing.

Material	Brittleness, B	
	[10 ¹⁰ /Pa%]	
	untreated	annealed
PLA	1.21	0.62
5BP	1.19	1.12
10BP	1.18	1.12
20BP	0.99	1.26
5BMF	1.16	0.58
10BMF	1.16	0.60
20BMF	0.93	0.60

Writing - review & editing, Resources, Investigation. **Olga Mysiukiewicz**: Investigation, Formal analysis, Validation, Writing - review & editing. **Danuta Matykievicz**: Investigation, Resources. **Arkadiusz Kloziński**: Investigation. **Jacek Andrzejewski**: Investigation. **Adam Piasecki**: Investigation, Visualization.

Acknowledgments

This study was supported by the National Center for Research and Development of Poland under project LIDER/25/0148/L-8/16/NCBR/2017 "Development of hybrid biodegradable composites' manufacturing technology for the automotive industry".

Appendix A. Supplementary data

Supplementary data to this article can be found online at <https://doi.org/10.1016/j.polymertesting.2020.106628>.

References

- [1] S. Farah, D.G. Anderson, R. Langer, Physical and mechanical properties of PLA, and their functions in widespread applications — a comprehensive review, *Adv. Drug Deliv. Rev.* 107 (2016) 367–392, <https://doi.org/10.1016/j.addr.2016.06.012>.
- [2] P. Siwek, I. Domagała-Świątkiewicz, P. Bucki, M. Puchalski, Biodegradable agroplastics in 21st century horticulture, *Polimery* 64 (2019) 480–486, <https://doi.org/10.14314/polimery.2019.7.2>.
- [3] W. Sikorska, M. Musiol, J. Rydz, M. Kowalczyk, G. Adamus, Kompostowanie przemysłowe jako metoda zagospodarowania odpadów z materiałów poliestrowych otrzymanych z surowców odnawialnych, *Polimery* 64 (2019) 818–827, <https://doi.org/10.14314/polimery.2019.11.11>.
- [4] K. Moraczewski, R. Malinowski, W. Sikorska, T. Karasiewicz, M. Stepczyńska, B. Jagodziński, P. Rytlewski, Composting of polylactide containing natural antiaging compounds of plant origin, *Polymers* 11 (2019) 1582, <https://doi.org/10.3390/polym11101582>.
- [5] E. Castro-Aguirre, F. Iniguez-Franco, H. Samsudin, X. Fang, R. Auras, Poly(lactic acid)—mass production, processing, industrial applications, and end of life, *Adv. Drug Deliv. Rev.* 107 (2016) 333–366, <https://doi.org/10.1016/j.addr.2016.03.010>.
- [6] M. Murariu, P. Dubois, PLA composites: from production to properties, *Adv. Drug Deliv. Rev.* 107 (2016) 17–46, <https://doi.org/10.1016/j.addr.2016.04.003>.
- [7] K. Oksman, M. Skrifvars, J.-F. Selin, Natural fibres as reinforcement in poly(lactic acid) (PLA) composites, *Compos. Sci. Technol.* 63 (2003) 1317–1324, [https://doi.org/10.1016/S0266-3538\(03\)00103-9](https://doi.org/10.1016/S0266-3538(03)00103-9).
- [8] D. Battagazzore, J. Alongi, A. Frache, Poly(lactic acid)-based composites containing natural fillers: thermal, mechanical and barrier properties, *J. Polym. Environ.* 22 (2014) 88–98, <https://doi.org/10.1007/s10924-013-0616-9>.
- [9] D. Battagazzore, S. Bocchini, J. Alongi, A. Frache, Rice husk as bio-source of silica: preparation and characterization of PLA-silica bio-composites, *RSC Adv.* 4 (2014) 54703–54712, <https://doi.org/10.1039/C4RA05991C>.
- [10] B. Bax, J. Müssig, Impact and tensile properties of PLA/Cordenka and PLA/flax composites, *Compos. Sci. Technol.* 68 (2008) 1601–1607, <https://doi.org/10.1016/j.compscitech.2008.01.004>.
- [11] D. Battagazzore, A. Noori, A. Frache, Natural wastes as particle filler for poly(lactic acid)-based composites, *J. Compos. Mater.* 53 (2019) 783–797, <https://doi.org/10.1177/0021998318791316>.
- [12] D. Battagazzore, S. Bocchini, J. Alongi, A. Frache, Plasticizers, antioxidants and reinforcement fillers from hazelnut skin and cocoa by-products: extraction and use in PLA and PP, *Polym. Degrad. Stabil.* 108 (2014) 297–306, <https://doi.org/10.1016/j.polymdegradstab.2014.03.003>.
- [13] L.-T. Lim, R. Auras, M. Rubino, Processing technologies for poly(lactic acid), *Prog. Polym. Sci.* 33 (2008) 820–852, <https://doi.org/10.1016/j.progpolymsci.2008.05.004>.
- [14] X. Shi, G. Zhang, T. Phuong, A. Lazzeri, Synergistic effects of nucleating agents and plasticizers on the crystallization behavior of poly(lactic acid), *Molecules* 20 (2015) 1579–1593, <https://doi.org/10.3390/molecules20011579>.
- [15] Z. Wei, P. Song, C. Zhou, G. Chen, Y. Chang, J. Li, W. Zhang, J. Liang, Insight into the annealing peak and microstructural changes of poly(l-lactic acid) by annealing at elevated temperatures, *Polymer* 54 (2013) 3377–3384, <https://doi.org/10.1016/j.polymer.2013.04.027>.
- [16] L. Yi, J. Zhang, J. Yang, F. Sun, H. Zhang, L. Zhao, Effect of annealing induced crystalline evolution on the scratch resistance of polylactide, *Tribol. Int.* 128 (2018) 328–336, <https://doi.org/10.1016/j.triboint.2018.07.041>.
- [17] D.K. Debeli, M. Tebyetekerwa, J. Hao, F. Jiao, J. Guo, Improved thermal and mechanical performance of ramie fibers reinforced poly(lactic acid) biocomposites via fiber surface modifications and composites thermal annealing, *Polym. Compos.* 39 (2018) E1867–E1879, <https://doi.org/10.1002/pc.24844>.
- [18] Y. Srithep, P. Nealey, L.-S. Turng, Effects of annealing time and temperature on the crystallinity and heat resistance behavior of injection-molded poly(lactic acid), *Polym. Eng. Sci.* 53 (2013) 580–588, <https://doi.org/10.1002/pen.23304>.
- [19] T.-C. Yang, K.-C. Hung, T.-L. Wu, T.-M. Wu, J.-H. Wu, A comparison of annealing process and nucleating agent (zinc phenylphosphonate) on the crystallization, viscoelasticity, and creep behavior of compression-molded poly(lactic acid) blends, *Polym. Degrad. Stabil.* 121 (2015) 230–237, <https://doi.org/10.1016/j.polymdegradstab.2015.09.012>.
- [20] F. Ge, X. Wang, X. Ran, Effect of annealing on the properties of polylactide/poly(butylene carbonate) blend, *Adv. Polym. Technol.* 37 (2018) 1335–1344, <https://doi.org/10.1002/adv.21792>.
- [21] J. Wootthikanokkhan, T. Cheachun, N. Sombatsompop, S. Thumsorn, N. Kaabuthong, N. Wongta, J. Wong-On, S.I. Na Ayutthaya, A. Kositchaiyong, Crystallization and thermomechanical properties of PLA composites: effects of additive types and heat treatment, *J. Appl. Polym. Sci.* 129 (2013) 215–223, <https://doi.org/10.1002/app.38715>.
- [22] M.W. Kim, Y.S. Song, J.R. Youn, Effects of interfacial adhesion and crystallization on the thermoresistance of poly(lactic acid)/mica composites, *Compos. Part A Appl. Sci. Manuf.* 41 (2010) 1817–1822, <https://doi.org/10.1016/j.compositesa.2010.08.016>.
- [23] K. Piekarska, E. Piorkowska, J. Bojda, The influence of matrix crystallinity, filler grain size and modification on properties of PLA/calcium carbonate composites, *Polym. Test.* 62 (2017) 203–209, <https://doi.org/10.1016/j.polymertesting.2017.06.025>.
- [24] E. Picard, E. Espuche, R. Fulchiron, Effect of an organo-modified montmorillonite on PLA crystallization and gas barrier properties, *Appl. Clay Sci.* 53 (2011) 58–65, <https://doi.org/10.1016/j.clay.2011.04.023>.
- [25] V. Fiore, T. Scalici, G. Di Bella, A. Valenza, A review on basalt fibre and its composites, *Compos. B Eng.* 74 (2015) 74–94, <https://doi.org/10.1016/j.compositesb.2014.12.034>.
- [26] T. Tabi, P. Tamas, J.G. Kovacs, Chopped basalt fibres: a new perspective in reinforcing poly(lactic acid) to produce injection moulded engineering composites from renewable and natural resources, *Express Polym. Lett.* 7 (2013) 107–119, <https://doi.org/10.3144/expresspolymlett.2013.11>.
- [27] S. Kuciel, A. Kufel, Novel hybrid composites based on polypropylene with basalt/carbon fiber (Rapid communication), *Polimery* 63 (2018) 387–390, <https://doi.org/10.14314/polimery.2018.5.8>.
- [28] L. Han, F. Ma, S. Chen, Y. Pu, Effect of short basalt fibers on durability, mechanical properties, and thermal properties of poly(lactic acid) composites, *Polym. Renew. Resour.* 10 (2019) 45–59, <https://doi.org/10.1177/2041247919863631>.
- [29] Z. Yang, J. Liu, F. Wang, S. Li, X. Feng, Effect of fiber hybridization on mechanical performances and impact behaviors of basalt fiber/UHMWPE fiber reinforced epoxy composites, *Compos. Struct.* 229 (2019), <https://doi.org/10.1016/j.compstruct.2019.111434>, 111434.
- [30] W. Chen, H. Shen, M.L. Auaq, C. Huang, S. Nutt, Basalt fiber-epoxy laminates with functionalized multi-walled carbon nanotubes, *Compos. Part A Appl. Sci. Manuf.* 40 (2009) 1082–1089, <https://doi.org/10.1016/j.compositesa.2009.04.027>.
- [31] Z. Ying, D. Wu, M. Zhang, Y. Qiu, Polylactide/basalt fiber composites with tailorable mechanical properties: effect of surface treatment of fibers and annealing, *Compos. Struct.* 176 (2017) 1020–1027, <https://doi.org/10.1016/j.compstruct.2017.06.042>.
- [32] T. Tábi, P. Bakonyi, S. Hajba, P. Herrera-Franco, T. Czigány, J. Kovács, Creep behaviour of injection-moulded basalt fibre reinforced poly(lactic acid) composites, *J. Reinforc. Plast. Compos.* 35 (2016) 1600–1610, <https://doi.org/10.1177/0731684416661239>.
- [33] T. Tábi, M. Zarelli, Development of poly(lactic acid) filled with basalt fibres and talc for engineering applications, *Mater. Sci. Forum* 885 (2017) 303–308, <https://doi.org/10.4028/www.scientific.net/MSF.885.303>.
- [34] A. Zotti, S. Zuppolini, T. Tábi, M. Grasso, G. Ren, A. Borriello, M. Zarelli, Effects of 1D and 2D nanofillers in basalt/poly(lactic acid) composites for additive manufacturing, *Compos. B Eng.* 153 (2018) 364–375, <https://doi.org/10.1016/j.compositesb.2018.08.128>.
- [35] M.D. Samper, R. Petrucci, L. Sanchez-Nacher, R. Balart, J.M. Kenny, Properties of composite laminates based on basalt fibers with epoxidized vegetable oils, *Mater. Des.* 72 (2015) 9–15, <https://doi.org/10.1016/j.matdes.2015.02.002>.
- [36] D. Matykievicz, M. Barczewski, H. Pucala, Influence of the compression molding temperature on thermomechanical properties of the basalt-reinforced poly(Lactic acid) (PLA) composites, *Rev. Rom. Mater. Rom. J. Mater.* 48 (2018) 108–114.
- [37] M.T. Isa, A.S. Ahmed, B.O. Aderemi, R.M. Taib, I.A. Mohammed-Dabo, Effect of fiber type and combinations on the mechanical, physical and thermal stability properties of polyester hybrid composites, *Compos. B Eng.* 52 (2013) 217–223, <https://doi.org/10.1016/j.compositesb.2013.04.018>.
- [38] M. Barczewski, D. Matykievicz, O. Mysiukiewicz, P. Maciejewski, Evaluation of polypropylene hybrid composites containing glass fiber and basalt powder, *J. Polym. Eng.* 38 (2018) 281–289, <https://doi.org/10.1515/polyeng-2017-0019>.
- [39] D. Matykievicz, M. Barczewski, D. Knapki, K. Skórczewska, Hybrid effects of basalt fibers and basalt powder on thermomechanical properties of epoxy composites, *Compos. B Eng.* 125 (2017) 157–164, <https://doi.org/10.1016/j.compositesb.2017.05.060>.
- [40] D. Matykievicz, M. Barczewski, S. Michałowski, Basalt powder as an eco-friendly filler for epoxy composites: thermal and thermo-mechanical properties assessment, *Compos. B Eng.* 164 (2019) 272–279, <https://doi.org/10.1016/j.compositesb.2018.11.073>.
- [41] M. Kurańska, M. Barczewski, K. Uram, K. Lewandowski, A. Prociak, S. Michałowski, Basalt waste management in the production of highly effective porous polyurethane composites for thermal insulating applications, *Polym. Test.* 76 (2019) 90–100, <https://doi.org/10.1016/j.polymertesting.2019.02.008>.

- [42] P. McKeown, S.N. McCormick, M.F. Mahon, M.D. Jones, Highly active Mg(ii) and Zn(ii) complexes for the ring opening polymerisation of lactide, *Polym. Chem.* 9 (2018) 5339–5347, <https://doi.org/10.1039/C8PY01369A>.
- [43] M. Nofar, R. Salehiyan, S. Sinha Ray, Rheology of poly (lactic acid)-based systems, *Polym. Rev.* 59 (2019) 465–509, <https://doi.org/10.1080/15583724.2019.1572185>.
- [44] M. Barczewski, K. Salasińska, A. Kloziński, K. Skórczewska, J. Szulc, A. Piasecki, Application of the basalt powder as a filler for polypropylene composites with improved thermo-mechanical stability and reduced flammability, *Polym. Eng. Sci.* 59 (2019) E71–E79, <https://doi.org/10.1002/pen.24962>.
- [45] M. Barczewski, K. Biedrzycka, O. Mysiukiewicz, D. Matykiewicz, J. Andrzejewski, A. Kloziński, M. Szostak, Milled basalt fibers as reinforcement for polyurea composite spray coatings with improved thermomechanical stability and mechanical performance, *Polimery* 65 (2020) 184–195, <https://doi.org/10.14314/polimery.2020.3.3>.
- [46] P. Pan, Y. Inoue, Polymorphism and isomorphism in biodegradable polyesters, *Prog. Polym. Sci.* 34 (2009) 605–640, <https://doi.org/10.1016/j.progpolymsci.2009.01.003>.
- [47] J. Zhang, K. Tashiro, H. Tsuji, A.J. Domb, Disorder-to-order phase transition and multiple melting behavior of poly(L-lactide) investigated by simultaneous measurements of WAXD and DSC, *Macromolecules* 41 (2008) 1352–1357, <https://doi.org/10.1021/ma0706071>.
- [48] E.W. Fischer, H.J. Sterzel, G. Wegner, Investigation of the structure of solution grown crystals of lactide copolymers by means of chemical reactions, *Kolloid-Z. Z. Polym.* 251 (1973) 980–990, <https://doi.org/10.1007/BF01498927>.
- [49] W. Brostow, H.E. Hagg Lobland, M. Narkis, Sliding wear, viscoelasticity, and brittleness of polymers, *J. Mater. Res.* 21 (2006) 2422–2428, <https://doi.org/10.1557/jmr.2006.0300>.
- [50] S. Wong, R.A. Shanks, A. Hodzic, Poly(L-lactic acid) composites with flax fibers modified by plasticizer absorption, *Polym. Eng. Sci.* 43 (2003) 1566–1575, <https://doi.org/10.1002/pen.10132>.
- [51] T. Liu, X. Yu, F. Yu, X. Zhao, A. Lu, J. Wang, X. Wang, T. Liu, Isothermal crystallization kinetics of fiber/poly(lactic acid) composites and morphology, *Polym. Plast. Technol. Eng.* 51 (2012) 597–604, <https://doi.org/10.1080/03602559.2012.659309>.
- [52] H. Pan, Z. Cao, Y. Chen, X. Wang, S. Jia, H. Yang, H. Zhang, L. Dong, Effect of molecular stereoregularity on the transcrystallization properties of poly(L-lactide)/basalt fiber composites, *Int. J. Biol. Macromol.* 137 (2019) 238–246, <https://doi.org/10.1016/j.ijbiomac.2019.06.147>.
- [53] A. Banasiak, T. Sterzyński, Właściwości kompozytów polimerowych PE + Talk, *Kompozyty* 2 (2002) 126–130.
- [54] J.M. Fischer, *Handbook of Molded Part Shrinkage and Warpage*, Elsevier, 2013, <https://doi.org/10.1016/C2011-0-06800-X>.
- [55] W. Guo, B. Yang, R. Xia, L. Su, J. Miao, J. Qian, P. Chen, X. Yu, Q. Zhang, S. Deng, Three-dimensional simulation of the shrinkage behavior of injection-molded poly lactic acid (PLA): effects of temperature, shear rate and Part Thickness, *J. Res. Uplat. Polym. Sci.* 2 (2013) 168–173, <https://doi.org/10.6000/1929-5995.2013.02.03.4>.
- [56] T. Tabi, I.E. Sajo, F. Szabo, A.S. Luyt, J.G. Kovacs, Crystalline structure of annealed polylactic acid and its relation to processing, *Express Polym. Lett.* 4 (2010) 659–668, <https://doi.org/10.3144/expresspolymlett.2010.80>.
- [57] H. Cai, V. Dave, R.A. Gross, S.P. McCarthy, Effects of physical aging, crystallinity, and orientation on the enzymatic degradation of poly(lactic acid), *J. Polym. Sci., Part B: Polym. Phys.* 34 (1996) 2701–2708, [https://doi.org/10.1002/\(SICI\)1099-0488\(19961130\)34:16<2701::AID-POLB2>3.0.CO;2-S](https://doi.org/10.1002/(SICI)1099-0488(19961130)34:16<2701::AID-POLB2>3.0.CO;2-S).
- [58] M. Barletta, M. Puopolo, Thermo-mechanical properties of injection molded components manufactured by engineered biodegradable blends, *J. Polym. Environ.* 27 (2019) 2105–2118, <https://doi.org/10.1007/s10924-019-01500-4>.
- [59] M. Hrabalova, A. Gregorova, R. Wimmer, V. Sedlarik, M. Machovsky, N. Mundigler, Effect of wood flour loading and thermal annealing on viscoelastic properties of poly(lactic acid) composite films, *J. Appl. Polym. Sci.* 118 (2010) 1534–1540, <https://doi.org/10.1002/app.32509>, n/a-n/a.
- [60] D.M. Dean, A.A. Marchione, L. Rebenfeld, R.A. Register, Flexural properties of fiber-reinforced polypropylene composites with and without a transcrystalline layer, *Polym. Adv. Technol.* 10 (1999) 655–668, [https://doi.org/10.1002/\(SICI\)1099-1581\(199911\)10:11<655::AID-PAT919>3.0.CO;2-%23](https://doi.org/10.1002/(SICI)1099-1581(199911)10:11<655::AID-PAT919>3.0.CO;2-%23).
- [61] C. Benwood, A. Anstey, J. Andrzejewski, M. Misra, A.K. Mohanty, Improving the impact strength and heat resistance of 3D printed models: structure, property, and processing relationships during fused deposition modeling (FDM) of poly(lactic acid), *ACS Omega* 3 (2018) 4400–4411, <https://doi.org/10.1021/acsomega.8b00129>.
- [62] D. Battagazzore, S. Bocchini, A. Frache, Crystallization kinetics of poly(lactic acid)-talc composites, *Express Polym. Lett.* 5 (2011) 849–858, <https://doi.org/10.3144/expresspolymlett.2011.84>.
- [63] R. Tokoro, D.M. Vu, K. Okubo, T. Tanaka, T. Fujii, T. Fujiura, How to improve mechanical properties of polylactic acid with bamboo fibers, *J. Mater. Sci.* 43 (2008) 775–787, <https://doi.org/10.1007/s10853-007-1994-y>.
- [64] W. Liu, M. Misra, P. Askeland, L.T. Drzal, A.K. Mohanty, 'Green' composites from soy based plastic and pineapple leaf fiber: fabrication and properties evaluation, *Polymer* 46 (2005) 2710–2721, <https://doi.org/10.1016/j.polymer.2005.01.027>.
- [65] S.F. Xavier, J.M. Schultz, K. Friedrich, Fracture propagation in particulate filled polypropylene composites, *J. Mater. Sci.* 25 (1990) 2411–2420, <https://doi.org/10.1007/BF00638035>.
- [66] P.S. Theocaris, G.C. Papanicolaou, G.A. Papadopoulos, The effect of filler-volume fraction on crack-propagation behavior of particulate composites, *J. Compos. Mater.* 15 (1981) 41–54, <https://doi.org/10.1177/002199838101500104>.
- [67] P. Xie, G. Wu, Z. Cao, Z. Han, Y. Zhang, Y. An, W. Yang, Effect of mold opening process on microporous structure and properties of microcellular polylactide–polylactide Nanocomposites, *Polymers* 10 (2018) 554, <https://doi.org/10.3390/polym10050554>.
- [68] J. Xu (Ed.), *Microcellular Injection Molding*, John Wiley & Sons, Inc., Hoboken, NJ, USA, 2010, <https://doi.org/10.1002/9780470642818>.
- [69] M. Bramuzzo, A. Savadori, D. Bacci, Polypropylene composites: fracture mechanics analysis of impact strength, *Polym. Compos.* 6 (1985) 1–8, <https://doi.org/10.1002/pc.750060102>.
- [70] A. Hejna, M. Sulyman, M. Przybysz, M.R. Saeb, M. Klein, K. Formela, On the correlation of lignocellulosic filler composition with the performance properties of poly(ϵ -caprolactone) based biocomposites, *Waste and Biomass Valorization* 11 (2020) 1467–1479, <https://doi.org/10.1007/s12649-018-0485-5>.
- [71] I. El Aboudi, A. Mdarhri, C. Brosseau, A. Montagne, F. Elhaouzi, Z. Bouyahia, A. Iost, Investigating carbon-black-filled polymer composites' brittleness, *Polym. Bull.* (2019), <https://doi.org/10.1007/s00289-019-03000-w>.